Wiley
International Journal of Chemical Engineering
Volume 2025, Article ID 1707820, 16 pages
https://doi.org/10.1155/ijce/1707820

WILEY

Research Article

Electrochemical Remediation of Marine Sediments Spiked With Hg and PAHs: Comparison of the Enhancing Agents' Nature

Federica Proietto,[1] **Claudia Prestigiacomo**,[1] **Fabio D'Agostino**,[2] **Maria Bonsignore**,[2] **Mario Sprovieri**,[3] **Alessandro Galia**,[1] **and Onofrio Scialdone**[1]

[1]*Engineering Department, University of Palermo, Viale Delle Scienze, Ed. 6, Palermo 90128, Italy*
[2]*Institute of Anthropic Impacts and Sustainability in the Marine Environment (IAS), National Research Council of Italy (IAS-CNR), Via Del Mare 3, Torretta Granitola, Trapani 91021, Italy*
[3]*Institute of Marine Sciences (CNR-ISMAR), Tesa 104–Arsenale, Castello 2737/F, Venezia 930122, Italy*

Correspondence should be addressed to Federica Proietto; federica.proietto@unipa.it

Received 3 October 2024; Accepted 27 May 2025

Academic Editor: Nicole Vorhauer-Huget

Real marine sediments dredged from Capo Granitola (CG) (Sicily, Italy) artificially contaminated were treated via an electrokinetic (EK) process. Mercury (Hg) and phenanthrene (PHE) or a mixture of PAHs (to simulate a more complex site) were selected as models of heavy metals and organic hazardous compounds, respectively. The aim of this work was to systematically investigate the effect of different enhancing agents on the removal of both classes of contaminants. Marine sediments were treated using a three-compartment cell under 1 V cm^{-1} for 10 days. The usage of different enhancing agents, including deionized water, trisodium N-(1-carboxylatoethyl)-iminodiacetate hydrate (MGDA) as chelating agents, Tween 80 surfactant and hydrogen peroxide, was investigated, to prompt the simultaneous removal of both classes of contaminants. The optimum option for the simultaneous removal was observed using a MGDA and Tween 80 solution as anolyte and MGDA solution as catholyte. These adopted conditions allow to reach the highest removal of Hg up to 22.5% and of PHE up to 62% in the case of the sediments contaminated with Hg and PHE and a total Hg removal of 13% coupled with a total PAHs removal of 45% in the case of sediments spiked with Hg and a mixture of five PAHs. It was observed that the nature of the enhancing agents used as electrolytes and their combination strongly affect the remediation treatment in terms of both distribution into the sediments and the total contaminants' removal.

Keywords: electrokinetic; Hg; marine sediments; PAHs; phenanthrene

1. Introduction

Over the last decades, direct current technologies (DCTs) have been explored as viable methods for the remediation of contaminated soils and marine sediments. The latter is considered one of the most crucial and challenging environmental issues [1]. The contamination of these sites is due mainly to anthropogenic actions, including accidental spills and/or inadequate management of hazardous substances [2, 3]. The Italian government identified 39 Sites of National Interest (SIN) in Italy (MATTM, DM 2013). These are complex sites characterized by fine grains, low hydraulic permeability and the presence of many hazardous organic (i.e., polycyclic aromatic hydrocarbons (PAHs), PCBs, HCB and TPHs) and inorganic (i.e., Hg, As, Pb, Cr and Zn) contaminants at elevated concentration, which require imminent remediation. For these cases, DCTs are regarded as among the most cost-effective, sustainable, environmentally friendly, noninvasive and practical for both in situ and ex situ approaches with respect to the other investigated strategies (including thermal, electromagnetic, chemical, ultrasonic and biological).

By applying a cell potential between two or more electrodes that are directly inserted or adjacent to the contaminated site, the DCT treatment exposes the polluted media to an electric field (E), which causes a direct current flow through the sediments. Under these conditions, different mechanisms are established: electromigration (flow of charged species), electroosmosis (flow of pore water and contaminants), electrophoresis (movement of colloids) and redox reactions on soils/sediments' particles and/or at the electrodes, facilitating the remediation of contaminated sites [1, 4–6]. DCTs can be categorized as electrokinetics (EKs), when an E higher than or equal to $1\ V\ cm^{-1}$ is induced to the sediments, and electrochemical remediation technologies (ECRTs), when the E is below $1\ V\ cm^{-1}$; these technologies involve different operative mechanisms and outputs [1, 6, 7]. ECRTs include the electrochemical geo-oxidation (ECGO; $0.0025 < E < 0.25\ V\ cm^{-1}$) and the induced complexation, which mineralizes organics and complexes metal contaminants, respectively [1, 6, 7].

In the case of ECGO, although the involved reaction mechanism is not clarified yet, it was shown that, under suitable conditions, the use of low values of E allows to desorb, mobilize and also degrade in situ the organics [6, 8–10]. As an example, Proietto et al. demonstrated that ECGO technology can be a suitable way to treat clay kaolin or marine sediments for the in situ removal of phenolic compounds [8], saturated alkanes [9] or PAHs [10] using E values lower than $0.25\ V\ cm^{-1}$ without the generation of a secondary effluent and at low energetic consumption (EC). Conversely, EK technologies involve E typically higher than or equal to $1\ V\ cm^{-1}$ [6]. In EK, the removal of contaminants is attributed mainly to electromigration and electroosmosis transport [11]. In contaminated marine sediments, the mobility of PAHs and heavy metals is usually low, leading to a very slow remediation rate. Different works aimed to remove these contaminants from the sediments, transporting them towards the electrolyte external compartments using several enhancing agents and E of approximately $1\ V\ cm^{-1}$ [12–22]. Falciglia et al. [15] revealed that the simultaneous use of an anolyte based on MGDA and Tween 80 coupled with an EDTA catholyte solution, as enhancing agents, allowed to reach a removal of both Hg and total PAHs up to 60% after 240 h under $1.2\ V\ cm^{-1}$ and using stainless steel as electrodes. In particular, Tween 80, i.e., polyoxyethylene (20) sorbitan monooleate, is a nonionic surfactant that is not toxic and biodegradable demonstrating promising efficacy in the removal of PAHs [23]. Recently, Chu et al. [24] developed a novel EK-Fenton technology for the in situ production of H_2O_2, using a gas diffusion electrode and $1\ V\ cm^{-1}$, which resulted in a partial removal of anthracene, pyrene and benzanthracene (22%–64%) within 5 days.

The EK approach can be applied as in situ and ex situ technologies. Ex situ methods need additional costs for dredging sediments from the original sites increasing the risk of causing dispersion in the environment. This risk mostly occurs during the mobilization of contaminated sediments. The EK approaches as remediation strategies are well-established technologies for soil remediation, and only a few applications have demonstrated the scale-up applicability of this technique [25–29]. However, recent studies have shown that one of the main factors which limit EK application on a large scale is the low amount of research studies on the EK treatment of marine sediments (< 10% of the articles focussing on the remediation) [25]. The main challenges are associated with the in situ generation of chloride anions and the corrosive environment, which considerably increase the cost of the materials required as electrodes and involve complex technologies' design. Some unclear factors need to be examined in detail, such as the characterization of by-products, the production of toxic metabolites, the co-existence of different pollutants in soil and sediments (which can behave differently under electric fields), practical issues due to shortage of in situ equipment data from the applicative scale which are essential for modelling the process as well as for technical economic analysis [25, 29]. In addition, the larger the scale of electrical distribution, the higher the energy consumption per unit of volume of remediated sediment, the lower the removal of pollutants [30–32]. In this framework, all these aspects have to be investigated in order to overcome the main challenges of these technologies improving the technical–economic feasibility for their scalability on the large scale. One of these factors includes that the electrochemical treatment of contaminated sediments and soils strongly depends on their own characteristics on the nature of the pollutants and the interaction between them. This means that, for each site, there is a set of proper operative conditions that should be optimized.

According to these considerations, in the work herein, model marine sediments were artificially spiked in order to conduct a systematic investigation of the simultaneous treatment of heavy metals and organic hazardous compounds. Hg and PAHs were selected as models of heavy metals and organic hazardous compounds, respectively. The spiked marine sediments were treated for 10 days by EK adopting E equal to $1\ V\ cm^{-1}$ in the presence of electrode compartments and electrolyte solutions. This work aimed to investigate and compare the effect of different enhancing agents selected from the literature on the EK performances for the simultaneous removal of both inorganic and organic contaminants. Herein, the most appealing enhancing agents currently used for different kinds of soil and sediment were systematically used and compared for the first time to treat the same matrix of marine sediments. The performances of the EK treatment were discussed in terms of the distribution of each i-pollutant (C_i/C_i°) along the sediments and its total removal (R_i) from the sediments. To reach this goal, in the first stage, a simplified model matrix of clean and real marine sediment dredged from Capo Granitola (CG) Bay (in Italy) spiked by Hg and phenanthrene (PHE) was treated. Then, clean sediments spiked with a Hg and a mixture of five PAHs (fluorene—FLU, PHE, benzo(a)pyrene—BAP, benzo(ghi) perylene—BPR, indeno(1,2,3-cd)pyrene—INP) were treated to simulate a more complex site.

2. Materials and Methods

2.1. Chemicals. Ultrapure water with a purity HPLC grade (CAS N. 7732-18-5) supplied by Sigma-Aldrich was used to set the moisture of the sediments. Sediments were spiked

using model organic and inorganic pollutants. Mercury (II) dinitrate in water solution (Hg standard for ICP/MS, CAS N. 10045-94-0) supplied by Carbo Erba was used as the model inorganic persistent contaminant, while a mixture of five PAHs congeners created ad hoc in acetone, i.e., FLU, PHE, BPA, BPR, INP, as a hazardous model for persistent organic PAHs. In addition, a mix of deuterated PAHs (acenaphtyleneD8, pyreneD10, benzo(a)pyreneD12) was used to fine-tune the gas chromatography–mass spectroscopy (GC/MS). Acetone (HPCL grade, Carlo Erba) and hexane (Pesticides grade, Sigma-Aldrich) were adopted to perform PAHs solid–liquid extraction from the dried sediment samples. EK treatments were performed using compact graphite (Carlo Erba-Reagents) as electrode material. Tween 80 (polyoxyethylene (20) sorbitan monooleate) supplied by Sigma-Aldrich was used as nonionic surfactant. Trisodium N-(1-carboxylatoethyl)-iminodiacetate hydrate (purity > 95% $C_7H_8NNa_3O_6$ xH_20 CAS N. 164462-16-2) (MGDA) supplied by TCI, Ltd. was used as chelating agent. Hydrogen peroxide 30% w/w H_2O_2 was supplied by Riedel-d Haen.

2.2. Physical and Chemical Characterization of Spiked Marine Sediments. Clay marine sediments dredged from CG Coast (province of Trapani), sited in the western of Sicily, in Italy, were used for this work (N 37°33.895′, E 12°39.626′, N 37°30.941′ and E 12°33.263′). Clean and real marine sediment was artificially contaminated following the OECD guidelines (OECD Guidelines, 2007). Sediments were artificially spiked with Hg and PHE or a mixture of five PAHs (FLU, PHE, BPA, BPR and INP) since they are the main compounds of real marine sediments dredges from Augusta Bay in the south of Sicily (Syracuse, Italy) [10] to simulate a real case study. The concentrations of Hg and PHE were the same in both Hg/PHE and Hg/five PAHs spiked sediments. Before the sediments' characterization, they were kept for 6 months in a freezer. Table 1 reports the physical and chemical features of the spiked sediments and the followed methods for their determination. In this context, it is complicated to predict how the results could be different or how the performances of the process could be affected when real contaminated marine sediments are treated under the same operative condition. However, artificially spiked marine sediments with model contaminants were treated in this work since the literature reveals that the scaling-up of this technology needs a step-by-step investigation in which different scales (i.e., simple laboratory, bench, pilot up to a prototype) contribute with pieces of relevant and non-overlapping information [33]. Sediments (500 g) were spiked with 3 mL of 1000 mg L^{-1} of Hg(II) standard water solutions. Sediments were homogenized in a rotary vapour balloon for 2 h and then dried under vacuum. Subsequentially, 3 mL of an ad hoc solution of 1000 mg L^{-1} per each of five PAHs congeners (FLU, PHE, BPA, BPR and IND) in acetone was added to the sediments. Hence, they were again homogenized in a rotary vapour balloon for 2 h and then dried under vacuum. Lastly, these contaminated sediments (500 g) were blended with other clean and dried sediments (2500 g). Then, they were placed in a rotary bottle of 10 L, closed and homogenized for 10 h. Hence, to amplify the interactions between the sediments and the contaminants, spiked dried sediments were stored at 4°C for 6 months.

2.3. EK Treatments. The electrochemical cell used in this work was described by Proietto et al. [10]. Briefly, the homemade Plexiglas cell (Figure 1) comprises three compartments: two external chambers where the processing fluids and electrodes were placed and a middle compartment where spiked sediments were located. Graphite electrodes with a working area of 4 cm^2 were selected as electrode material at both the anode and the cathode side. According to the literature, compact graphite is cost-effective, environmentally friendly, has a good conductivity and does not require complex treatment with respect to the other kinds of electrodes (such as the couple DSA/Pt that is more expensive materials or stainless steel electrodes that need anticorrosion treatment) [8]. The distance between the electrodes was 10 cm. Sediments (100 g with a moisture content of 50%) were placed inside the cell layer by layer, pressed and packed down to avoid the presence of void spaces during an extended time of 12 h. The middle section was provided with a Plexiglass cover to limit the water evaporation and separated from the two external chambers by filter paper Whatman Qualitative, grade 1, circle 47 mm. At the end of each EK test, the cell was disassembled in each component and washed with deionized water (DW); the filter paper was removed discharged and replaced with a new one. The graphite electrodes were washed with DW, mechanically smoothed with abrasive paper and sonicated several times in DW for 10 min until the solution became clear and rinsed with DW. After each experiment, a degradation of the anode electrode was observed due to the presence of thin and small black particles of graphite in the anolyte. For all the experiments done in this study, the anolyte and catholyte solutions after electrolysis were not analysed, except in the case of EK1 test. In the latter case, both anolyte and catholyte were analysed.

Before each electrolysis, at least 3 samples of the sediment already placed in the middle sections were analysed to check the initial concentration of the contaminants, pH sediment and moisture. Table 2 reports the experimental trials performed in this study. EKC1 and EKC2 are two control tests (blank) performed for comparison over 10 days without the application of a cell potential ($E = 0$ V cm^{-1}). During these control tests, approximately 96% of the contaminants were recovered (coherently with the work's aim). The difference in the mass balance may be attributed to the possible contaminants' adsorption to the components of the electrochemical cell, including walls' cell, filter paper and sample vials.

EKC1 and EK1-EK5 trial numbers (Table 2) refer to the electrochemical treatment of the spiked sediments with Hg and PHE. These tests were planned to compare different processing fluids. DW was used in both anodic and cathodic chambers during EK1. An aqueous solution 0.1 M MGDA was used in both anodic and cathodic chambers (namely

Table 1: Characterization of spiked marine sediments.

Physical properties		Method	Spiked marine sediments [10]
Specific gravity (at 20°C)		ASTM D854-92	2.53
Sediment pH (ratio sediment/water of 1:5)		ISO 10390:2021	7.30
Moisture content (%)		ASTM D2974-14	50 ± 3.0
Organic matter (%)		ASTM D2974-14	10 ± 0.19
Particle size distribution (%)			
Clay		Horiba Partica LA-950V2 laser particle size analyser[a]	56.9 ± 0.9
Silt			42.3 ± 0.9
Sand			0.86 ± 0.2
Heavy metals[a]			
Mercury	Hg	US-EPA-7473	mg kg^{-1} 1.17
Polycyclic aromatic hydrocarbons (PAHs)[a]			
Congeners	Acronyms		μg kg^{-1}
Fluorene	FLU		112
Phenanthrene	PHE		353
Benzo(a)pyrene	BAP	GC/MS refers to Section 2.4	748
Benzo(ghi)perylene	BPR		1036
Indeno(1,2,3-cd)pyrene	INP		1036

[a]All these concentration values are the average of 10 replicated with a deviation standard close to 10%.

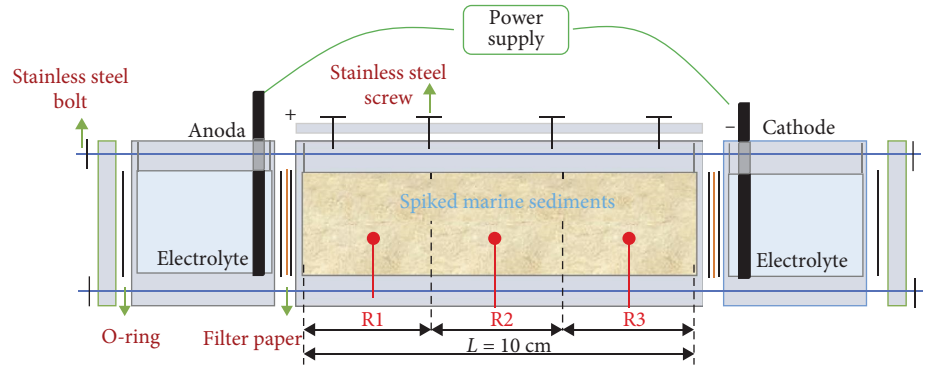

Figure 1: Schematic view of EK cell for the electrochemical treatment.

MGDA) during EK2; MGDA was selected with the aim to remove Hg since, according to the literature, it has shown a good chelating propriety and is easy biodegradable [15]. An aqueous solution 0.1M MGDA and 3 g L^{-1} (2.2 mM) of Tween 80 were used in both anodic and cathodic chambers (namely T + MGDA) during EK3; Tween 80 (polyoxyethylene (20) sorbitan monooleate), a nonionic surfactant, was selected to aid the PAHs removal since it is not toxic and biodegradable and has shown a possibility to remove PAHs [23], as already mentioned in the introduction section. Tween 80 has a molecular mass of 1310 g mol^{-1} and a critical micellar concentration (CMC) of 0.012 mM [34]. A combination of an aqueous solution 0.1 M MGDA and 3 g L^{-1} of Tween 80 (T + MGDA) and an aqueous solution 0.1 M MGDA (MGDA) were used as anolyte and catholyte, respectively, in EK4. An aqueous solution of 10% v/v H_2O_2 and 0.1 M MGDA (namely H_2O_2 + MGDA) was used in EK5, with the aim to simultaneously convert PAHs thanks to the oxidant action of the H_2O_2 and remove Hg thanks to the presence of MGDA.

EKC2 and EK6-EK7 trial numbers refer to the electrochemical treatment of the spiked sediments with Hg and the mixture of five PAH congeners. EK6 was performed by using DW as processing fluid and EK7 by using T + MGDA as anolyte and MGDA as catholyte.

EK1-EK7 electrolyses were performed at 1 V cm^{-1} using an AMEL 2549 potentiostat/galvanostat over a 10-day period at ambient temperature.

At the end of the treatment, three different samples of sediments were collected and characterized. The three different sampling points are shown in Figure 1, and they are termed R1 (near the anode), R2 (in the middle) and R3 (near the cathode). Moisture content, pH of each solid sample and residual content of sediment's contaminants were quantified. At least three sediment samples of the sediment already placed in the middle sections were analysed to check the

Table 2: Summary of experimental conditions.

Run	Anolyte	Sediment	Catholyte	Time (days)	E ($V\,cm^{-1}$)	Target
EKC1	Deionized water (DW)	Sediments spiked with Hg and PHE	Deionized water (DW)	10	0	Hg + PHE
EK1	Deionized water (DW)	Sediments spiked with Hg and PHE	Deionized water (DW)	10	1	Hg + PHE
EK2	0.1 M MGDA aqueous solution (MGDA)	Sediments spiked with Hg and PHE	0.1 M MGDA aqueous solution (MGDA)	10	1	Hg + PHE
EK3	3 $g{\cdot}L^{-1}$ Tween 80 and 0.1 M MGDA aqueous solution (T + MGDA)	Sediments spiked with Hg and PHE	3 g/L Tween 80 and 0.1 M MGDA aqueous solution (T + MGDA)	10	1	Hg + PHE
EK4	3 $g{\cdot}L^{-1}$ Tween 80 and 0.1 M MGDA aqueous solution (T + MGDA)	Sediments spiked with Hg and PHE	0.1 M MGDA aqueous solution (MGDA)	10	1	Hg + PHE
EK5	10% v/v H_2O_2 and 0.1 M MGDA aqueous solution (H_2O_2 + MGDA)	Sediments spiked with Hg and PHE	10% v/v H_2O_2 and 0.1 M MGDA aqueous solution (H_2O_2 + MGDA)	10	1	Hg + PHE
EKC2	Deionized water (DW)	Sediments spiked with Hg and a mixture of 5 PAHs	Deionized water (DW)	10	0	Hg + 5 PAHs
EK6	Deionized water (DW)	Sediments spiked with Hg and a mixture of 5 PAHs	Deionized water (DW)	10	1	Hg + 5 PAHs
EK7	3 $g{\cdot}L^{-1}$ Tween 80 and 0.1 M MGDA aqueous solution (T + MGDA)	Sediments spiked with Hg and a mixture of 5 PAHs	0.1 M MGDA aqueous solution (MGDA)	10	1	Hg + 5 PAHs

initial concentration of the contaminants, pH sediment and moisture. Electrolyses were performed at least two times to ensure the repeatability of the treatment. Analytical procedures were performed in triplicate, and the data are shown as the average of them.

2.4. Analytical Methods. US-EPA (7473) method was used to determine the total Hg content of each dried solid sample. Analytical procedures involved the following steps: an aliquot of ~0.05 g of dry sample was poured in nickel boats and directly transferred into the direct mercury analysers (DMA-80) (Milestone DMA-80 Tricell, Wesleyan University, Middletown, CT, USA) and then analysed for the Hg quantification. Hg determination in sediment samples was tested once every ten by analysing a Marine Sediment Certified Reference Material, namely PACS-3, produced by the National Research Council Canada (NRCC) (Canada) to conduct a quality control on the accuracy and precision (routinely) for DMA-80 instrument. Accuracy and precision were estimated to be between 94% and 109% and less than 7% (relative standard deviation (RSD%) on 5 replicates), respectively. Moreover, all the analyses for the Hg quantification were conducted in duplicate to evaluate the reproducibility of sediment samples (< 5%). To estimate the initial concentration of Hg (C°_{Hg}), ten aliquots of spiked sediments were measured.

PAHs concentration was evaluated by GC/MS. The concentration of the PAHs in the sediment samples was determined throughout a high-frequency sonication treatment with 20 kHz pulse frequency (activity 0.7 s (ON)–inactivity 0.3 s (OFF)), for at least 10 min with an 80% of the power, using a microwave probe (HD 2070 SONOPULS get by Bandelin, Germany) at directly immersed in a glass test tube containing 0.5 g of dry sample and 3 mL of liquid solution hexane/acetone 80:20 v/v. Consequently, a spoon of Na_2SO_4 anhydrous was added to the glass test tube and it was stirred by vortex for 1 min. The final suspension was centrifuged at 3000 rpm for 15 min in order to efficiently separate the solid sediment from the extractant liquid solution.

A cartridge CHROMABOND Florisil SPE (solid phase extraction sorbent in magnesium silicate) 200 mg/3 mL was used to purify the extracted solution, i.e., for the isolation of polar compounds from nonpolar matrices (EPA 3630C method). A BUCHI multivapour was used to dry the eluted solution, and then, 1 mL of hexane with an internal standard (at 200 μg mL^{-1} of PAH-mix9) was used to re-dissolve the residual phase. GC/MS equipped with a DB5-MS capillary column (30 m × 0.25 mm × 0.5 μm) in SIM mode was used to detect PAHs (EPA 8270D method). The GC/MS was set as follows: injector temperature of 280°C in a split-less mode; volume injected: 2 μL; the oven temperature follows (i) 60°C for 4 min, (ii) reaches 270°C at 10°C min^{-1} (hold for 5 min) and (iii) 340°C at 20°C min^{-1} (hold for 5 min). PHE was detected in the anolyte and the catholyte after EK1 run. GC/MS equipped with a DB5-MS capillary column (30 m × 0.25 mm × 0.5 μm) in SIM mode was used to detect PHE into the anolyte and catholyte (EPA 8270D method).

A Checker pH Tester (HI98103) HANNA instrument was used to measure the sediment pH by applying the ISO 10390:2021; for the pH measurement, a ratio between the sediment and the water of 1:5 was used. Moisture content (W) was quantified following the ASTM D2974-14.

2.5. Performance Metrics. The distribution of the *i*-contaminant along the Regions R1, R2 and R3 of the sediments (Figure 1) was reported and discussed considering the ratio between the final *i*-contaminant content (C_i) and the initial content (C°_i). For each EK treatment, to check whether the pollutants were homogeneously present in the treated bed, a certain amount of sample from Regions R1, R2 and R3 was taken, dried and then analysed following the procedure summarized in Section 2.4. The initial level of all the pollutants was approximately 1 ($C_i/C^{\circ}_i \sim 1 \pm 0.07$) at the beginning of the experiments.

The removal efficiency of each pollutant and the total PAHs removal from the sediments were computed by equations (1) and (2), respectively:

$$\text{Total } R_{i-\text{pollutant}}(\%) = \left(C^{o}_i - C^{f}_i\right)/C^{o}_i \times 100, \tag{1}$$

$$\text{Total } R_{\text{PAHs}}(\%) = \left(C^{o}_{\text{PAHs}} - C^{f}_{\text{PAHs}}\right)/C^{o}_{\text{PAHs}} \times 100, \tag{2}$$

where C^{o}_i and C^{f}_i are the initial and the final contents after 10 days (mg kg^{-1}) of each pollutant (i = Hg, FLU, PHE, BAP, BPR, INP) or PAHs per all the kg of dried treated sediments.

The EC was estimated by the following equation:

$$\text{EC}\left(\text{kWh kg}^{-1}\right) = \Delta V \times I \times t\,/w, \tag{3}$$

where I (A) is the current, t (s) is the treatment time, ΔV (V) is the applied cell potential, and w is the total quantity of sediment treatment (kg).

3. Results and Discussion

3.1. EK Treatment of Spiked Marine Sediments With Hg and Phenanthrene. To investigate the removal of Hg and PHE from marine sediments, a set of experiments was planned with the aim to study the effect of the nature of the electrolyte, including DW, MGDA, Tween 80, H_2O_2 and their combinations, on the EK performances. Table 2 in Section 2 reports in detail the used electrolyte and the experimental trials (EK1–EK5).

Figures 2 and 3 report the results of these trials in terms of the contaminant distribution along the regions R1, R2 and R3 of the middle compartment (C_i/C°_i) and the total removal of Hg and PHE from the sediments (R_i). The C_i/C°_i of Hg and PHE at the zero time was roughly 1, as a confirmation that Hg and PHE were equally distributed along the sediment bed (in Figures 2 and 3, $C_i/C^{\circ}_i \sim 1$ is indicated by a black dashed line—primary y-axis). All the EK experiments were carried out at 1 V cm^{-1} for 10 days using compact graphite as electrodes at ambient temperature and atmospheric pressure.

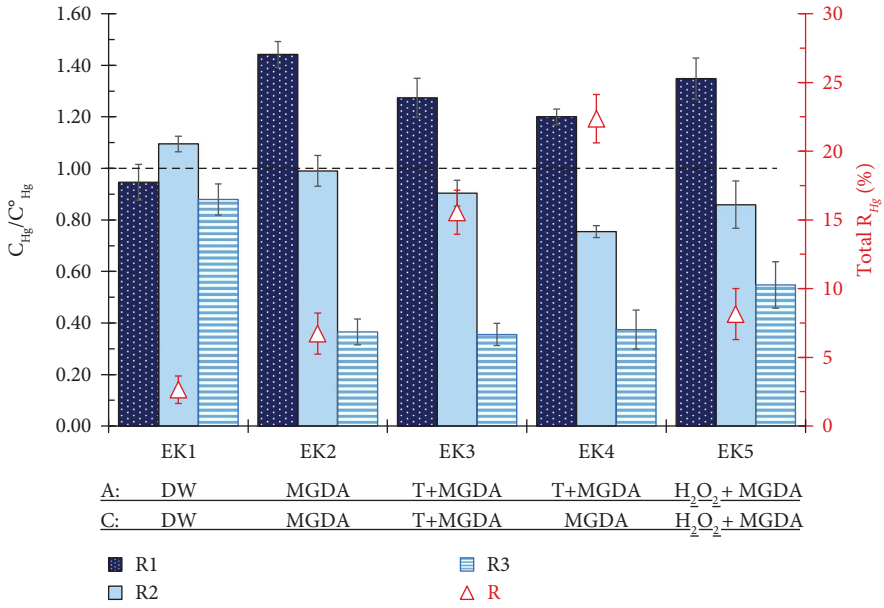

FIGURE 2: Final distribution of Hg (C_{Hg}/C°_{Hg}) along the treated sediment (R1, R2 and R3) (primary x-axis) and their total removal R_{Hg} (refers to red triangle symbol, △, secondary y-axis) in the EK1-EK6 runs. Black dashed line (---) indicates the initial normalized concentration ($C_{Hg}/C^{\circ}_{Hg} \sim 1$). A: Anolyte. C: Catholyte. DW: Deionized Water. MGDA: 0.1 M MGDA aqueous solution. T + MGDA: 3 g L^{-1} Tween 80 and 0.1 M MGDA aqueous solution. H_2O_2 + MGDA: 10% v/v H_2O_2 and 0.1 M MGDA aqueous solution. Electrolyses were performed under 1 V cm^{-1} for 10 days.

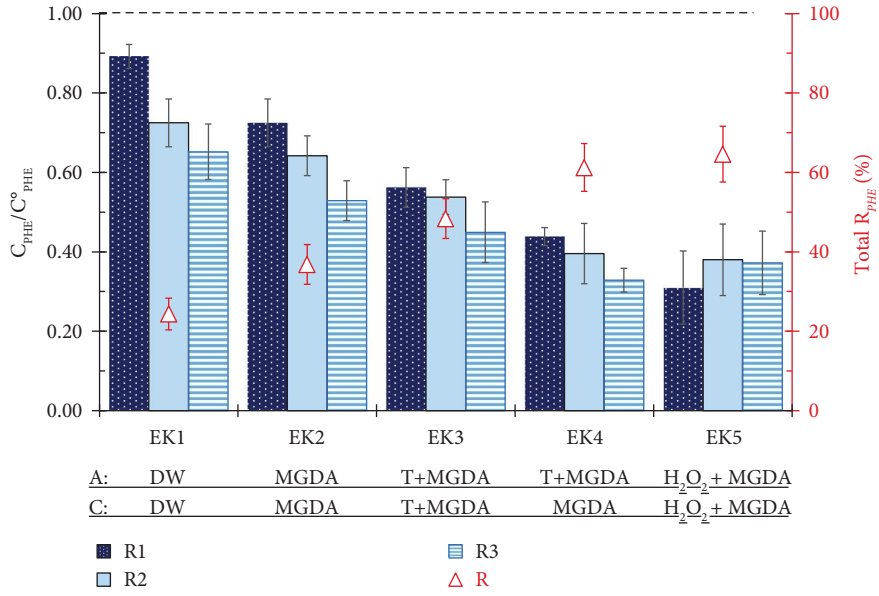

FIGURE 3: Final distribution of phenanthrene (C_{PHE}/C°_{PHE}) along the treated sediment (R1, R2 and R3) (primary x-axis) and their total removal R_{PHE} (refers to red triangle symbol, △, secondary y-axis) in the EK1-EK6 runs. Black dashed line (---) indicates the initial normalized concentration ($C_{PHE}/C^{\circ}_{PHE} \sim 1$). A: Anolyte. C: Catholyte. DW: Deionized Water. MGDA: 0.1 M MGDA aqueous solution. T + MGDA: 3 g L^{-1} Tween 80 and 0.1 M MGDA aqueous solution. H_2O_2 + MGDA: 10% v/v H_2O_2 and 0.1 M MGDA aqueous solution. Electrolyses were performed under 1 V cm^{-1} for 10 days.

First, experiments were performed using DW as both anolyte and catholyte (EK1). Following the EK1 treatment, it was observed that the distribution of Hg along the Regions R1, R2 and R3 does not appreciably change even if a little accumulation in Region R2 is observed, leading to a low value of R_{Hg} efficiency of approximately 2.5% (Figure 2 refers to the secondary y-axis). In the case of PHE, the ratio C_{PHE}/C°_{PHE} increased from Region R3 (cathode area) to Region R1 (anode area) and it was lower than 1, reaching a total R_{PHE} slightly higher than 21% (EK1, Figure 3 refers to the secondary y-axis).

To rationalize these data, it should be considered that when an E is induced in the sediment, different phenomena are involved in the process, such as electromigration, electroosmosis, electrophoresis and redox reaction at the electrodes [1]. The movement of the charged species towards the electrode with opposite polarity (i.e., positive ions move to the cathode and negative one towards the anode side) is due to the electromigration, while the movement of the pore fluid water and dissolved component within the porous of the sediments bed parallel to the applied E is due to the electroosmosis transport [29]. Typically, the induced E causes water to flow from the anode to the cathode side. However, if the surface charge varies or in the presence of humic substances that were reported to affect the mobilization of contaminants during EK treatment [14], the electroosmosis direction may be the opposite (from cathode to anode side). Instead, the redox processes at the electrodes compartment are mainly the H_2 evolution and O_2 generation at the cathode and anode side due to water electrolysis, respectively. In addition, at the anode compartment, it is expected that organics can be directly oxidized at the anode surface [35–37]. According to these considerations, the poor movement of Hg during EK1 can be attributed both to the neutrality charge of Hg present in the sediments and to its strong adsorption onto the sediment particles; hence, the induced E does not affect its removal. Conversely, the accumulation of PHE in the Region R1 and its partial removal from the sediments can be attributed to electroosmosis transport towards the anode compartments. PHE can be subsequently oxidized at the anode surfaces, ideally, leading to the formation of nontoxic products, such as carboxylic acids, or carbon dioxide and water. At the end of EK1 treatment, aliquots of both anolyte and catholyte were analysed to verify this hypothesis. Trace amounts of PHE were observed in the anolyte, while no PHE was revealed in the catholyte. Moreover, the redox process at the electrode leads to the generation of hydroxylic ions at the cathode and protons at the anode. These ions moved through the sediments via electromigration creating a difference in the sediment pH. Indeed, the pH values of the anolyte and the catholyte were approximately 1 and 14, respectively, and the pH sediments varied from 8.5 to 11.3 and 12.3 from Regions R1 to R2 and R3, respectively (Table 3, EK1). The slight pH change might be attributed to the high buffering capacity of the used sediments, as shown by Proietto et al. [10], which tends to hold out the alteration in pH.

To selectively improve the Hg mobilization, 0.1 M MGDA aqueous solutions were used as electrolyte fluid processes (EK2, Table 2). MGDA is a biodegradable chelating agent stable in a wide pH range [15]. Following the EK2 treatment, a drastic change in the distribution of Hg along the sediment was observed (Figure 2, EK2). C_{Hg}/C°_{Hg} increased from Region R3 (cathode compartment) to R1 (anode compartment), and it was higher than 1 in Region R1 ($C_{Hg}/C^{\circ}_{Hg} \sim 1.440$), close to 1 in R2 and lower than 1 in Region R3 ($C_{Hg}/C^{\circ}_{Hg} \sim 0.365$). The higher level of Hg at the anode side (R1) indicates that, under the adopted conditions, Hg was transported from Region R3 to R1, where it was accumulated. However, these conditions were not appropriate for the removal of Hg from the sediments; indeed, a total R_{Hg} of approximately 6% was observed (EK2, Figure 3 refers to the secondary y-axis). According to the literature [38, 39], MGDA acts as a chelating agent which generates Hg-MGDA stable complexes negatively charged (equation (4)) that are attracted by the positive electrode, thus causing the movement of the Hg towards the anode compartment:

$$M^{2+} + H_{gn}\text{MGDA}^{n-3} \longleftrightarrow \left[M\left(H_{gn}(\text{MGDA})\right)\right]^{n-2}, \quad n = 0, 1, 2. \tag{4}$$

Similar results were reported by Falciglia et al. [39] for the removal of Hg in real marine sediments under different conditions. They observed that the use of MGDA (5%) as anolyte and EDTA (0.1 M) as catholyte allowed to significantly change in the distribution of Hg along the sediments; they reached a total Hg removal of approximately 38% working in continuous electrolyte flow at 1.2 V cm^{-1} for 400 h using stainless steel electrodes. After EK2 treatment, a distribution of PHE similar to that of EK1 was observed (Figure 3, EK2); C_{PHE}/C°_{PHE} increased from Region R3 (cathode side) to R1 (anode side), and it was always lower than 1. However, the usage of MGDA gave a slight improvement in the PHE removal. Indeed, R_{PHE} of approximately 36% was reached (Figure 3, EK2 refers to the secondary y-axis). According to the literature, nonpolar molecules are not involved in the chelating process [14]. Hence, according to these considerations, the obtained results can be tentatively attributed to a synergic transport phenomenon of both the electroosmosis and the electromigration process caused by the movement of the Hg–MGDA–organic complexes towards the anode compartment, enhancing also the PHE transport. Also, in this case, a pH increase from the Region R1 (pH = 7) to R3 (pH = 12) (Table 3, EK2) was observed due to the electromigration phenomena occurring in EK processes.

Further experiments using nonionic surfactants were conducted to promote the mobilization of the organic contaminants adsorbed onto the sediments' particles. Among the surfactants used in the literature, Tween 80 has been widely used in soil remediation technologies thanks to its low toxicity, low cost and good biodegradability; moreover, it is characterized by a high solubility in water and low CMC (~0.012 mM) [15, 34, 40]. The surfactants at higher concentrations than the CMC create zones in water (namely micelles) in which organic compounds are highly soluble. A solution of Tween 80 at a concentration of 3 g L^{-1}, higher than the CMC, was used. Higher concentrations were not considered since the higher its concentration, the higher the viscosity solution, which can hinder the EK process performances [14]. When the Tween 80 surfactant was added to the electrolyte compartment (namely T + MGDA, Table 2) (EK3), an increase of both the removal of Hg and PHE was observed. More in detail, in both cases, similar distributions of Hg and PHE along the Regions R1, R2 and R3 with respect to the previous treatments were observed (Figures 2 and 3, EK3 primary y-axis) coupled with a drastic increase of the total R_{Hg} to 15.5% and of the total R_{PHE} to 50%

Table 3: pH values and total R_{PAHs} after the EK treatment[a].

Run	Anolyte[b]	Catholyte[b]	pH			Total R_{PAHs} (%)	EC (kWh kg^{-1})
			R1	R2	R3		
EK1	DW	DW	8.5	11.3	12.13	—	0.453
EK2	MGDA	MGDA	7.1	12.1	12.0	—	0.313
EK3	T + MGDA	T + MGDA	8.2	11.8	12.3	—	0.347
EK4	T + MGDA	MGDA	7.0	14.0	13.0	—	0.652
EK5	H_2O_2 + MGDA	H_2O_2 + MGDA	10.0	12.0	12.0	—	0.438
EK6	DW	DW	8.5	11.3	12.2	20	NA
EK7	T + MGDA	MGDA	8.0	11.8	11.8	45	NA

Abbreviation: DW = deionized water.

[a]Electrokinetic treatment was performed at 1 V cm^{-1} using compact graphite electrode. Treatment time 10 days.

[b]MGDA: 0.1 M MGDA aqueous solution; T + MGDA: 3 g L^{-1} Tween 80 and 0.1 M MGDA aqueous solution; H_2O_2 + MGDA: 10% v/v H_2O_2 and 0.1 M MGDA aqueous solution.

(Figures 2 and 3, EK3 secondary *y*-axis). Also, in this case, the pH ranged from 8 to 12 (pH 8.2 in R1, 11.7 in R2 and 12.3 in R3, Table 3) due to the redox processes at the electrodes. The collected outcomes suggested that it is plausible to assume that the drastic enhancement of the Hg removal can be attributed to the co-presence of MGDA and Tween 80. Indeed, we suppose that the Hg–MGDA–organic complexes can be firstly solubilized into the micelles and then transported towards the anode side. In the case of PHE, the higher R_{PHE} value achieved in EK3 was attributed to the presence of the micelle of Tween 80 in which PHE is highly soluble, thus increasing the removal of PHE towards the Region R1. Falciglia et al. [15] tested a solution of Tween 80 and MGDA as anolyte for the treatment of marine sediments of Augusta Bay (Syracuse, Italy) reaching a removal of approximately 60% of both Hg and PAHs contaminants. These are very appealing results which inspired the usage of MGDA and Tween 80 as enhancing agents for the treatment of spiked marine sediments in this work. The different performances can be attributed to several aspects, including (i) the different nature of the sediments (real contaminated marine sediments from the bay of Augusta (Syracuse, Italy) vs. clean and real marine sediment from the golf of CG (Trapani, Italy) artificially spiked with model hazardous compounds) and their chemicophysical properties (i.e., clay/silt/sand, organic, hydraulic permeability, pH and buffering capacity); (ii) the nature of the contaminants (miscellaneous of real and toxic heavy metals, PAHs, PCBs, etc., vs a mixture of Hg and PHE); (iii) different applied treatments in terms of electrolyte solution as well as different operative conditions. As a comparison, Falciglia et al. [15] used different enhancing agents in the electrode compartments, e.g., EDTA or MGDA or MGDA + Tween 80 solution as anolyte and always 0.1 M of EDTA as catholyte and operates at 1.2 V cm^{-1} using stainless steel electrodes. Instead, in this work, the same nature of enhancing agent was used as anolyte and catholyte (e.g., MGDA as anolyte and catholyte or MGDA + Tween 80 as anolyte and catholyte) for each experiment conducted at 1 V cm^{-1} using compact graphite electrodes.

Aiming to further improve the performances of the removal of both contaminants, the T + MDGA electrolyte was used as anolyte and MGDA as catholyte (EK4). This configuration was selected to increase the gradient concentration of Tween 80 along the sediments bed, which moves inside the sediments driven from the electroosmotic flow of pore water towards the cathode side (from visive inspection the level of the catholyte solution increased with time during the treatment). Under the adopted conditions, the same trend of concentration of both Hg and PHE was observed (Figures 2 and 3, EK4 primary *y*-axis). C_{Hg}/C°_{Hg} reached 1.20, 0.755 and 0.375 in Regions R1, R2 and R3, respectively, thus increasing the total R_{Hg} to approximately 22.5% (Figure 2, EK4), while C_{PHE}/C°_{PHE} was 0.440, 0.400 and 0.330 in Regions R1, R2 and R3, respectively, coupled with a total R_{PHE} of 62% (Figure 3, EK4). In addition, also in this case, trace amounts of PHE were detected in the anolyte and no PHE was observed in the catholyte solution, showing the migration of PHE towards the anode side and its oxidation. Figure 4 reports the recorded current during the EK treatment, which depend on the nature of the enhancing agents used and decrease upon increasing the time. The highest current was recorded during EK 4 run.

The usage of H_2O_2 for soil/sediment remediation was proposed by a few authors, and this approach was termed EK-Fenton process [16, 21, 41, 42]. In the case of EK5, solutions of 10% v/v of H_2O_2 and 0.1 MGDA were used as anolyte and catholyte. A total R_{Hg} of approximately 8.15% was observed (Figure 2, EK5 secondary *y*-axis) which is similar to that obtained in EK2 treatment. Hence, also in this case, the removal of Hg is attributed to the presence of MGDA, which forms Hg-MGDA negatively charged complexes attracted by the positive electrode. Conversely, a homogeneous distribution of C_{PHE}/C°_{PHE} close to 0.360 in each Region R1, R2 and R3 coupled with a slightly higher removal of PHE up to 65% with respect to the other EK treatments (Figure 3, EK5) was found. The higher R_{PHE} is attributed to the presence of H_2O_2 which is an oxidant able to react with organics; additionally, iron ions are present in the sediments, and it is expected the H_2O_2 reacts with them leading to the generation of hydroxylic radical HO• [43–45]. The latter has a higher oxidant power than native H_2O_2, thus increasing oxidation of the PHE contaminant. Paixão et al. reported a removal of hydrocarbons of approximately 27% after 15 days of the treatment of petroleum-spiked kaolin via EK-Fenton process under 1 V cm^{-1} [41]. In this framework, it is important to note that this approach prevents the production of secondary effluent with higher organic

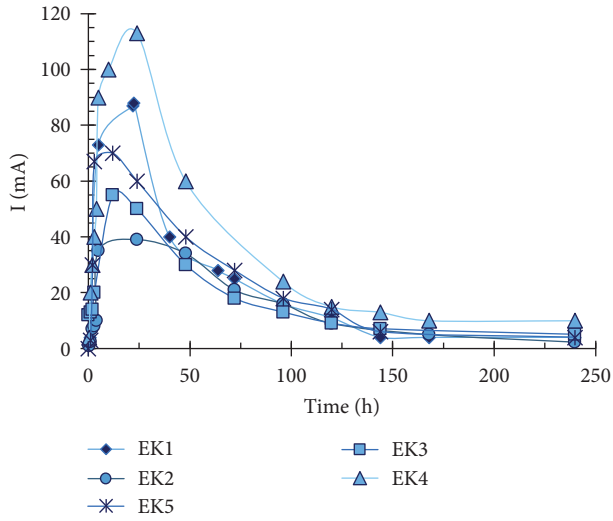

FIGURE 4: Plot of current intensity (I; mA) vs. time (hours) during the EK treatment summarized in Table 2. Electrolyses were performed under 1 V cm^{-1} for 10 days.

content, avoiding costs associated with its further treatment [21, 41, 42].

3.2. EK Treatment of Spiked Marine Sediments With Hg and Mixture of PAHs. According to the collected outcomes, the usage of T + MGDA solutions as electrolytes in both compartments gave rise to the highest performances for the removal of Hg and PHE with respect to the other strategies. Hence, to validate this approach for a more complex site, the sediments dredged from CG (Trapani, Italy) were artificially spiked with a mixture of Hg and five PAHs congeners (FLU, PHE, BAP, BPR and INP), namely, CG-MIX, and treated at 1 V cm^{-1} for 10 days using compact graphite as electrodes (Table 1).

In the first stage, the CG-MIX was treated using only DW as electrolyte in both compartments (EK6, Table 2). The results are reported in Figure 5. Also, in this case, the ratio C_i/C_i° of all the contaminants was approximately 1 at the zero time, highlighting that Hg and PAHs were homogeneously distributed in the sediments (Figure 5, $C_i/C_i^\circ \sim 1$, the black dashed line—primary y-axis). After the EK treatment, a similar scenario described in the EK1 (Figure 2) was observed for Hg. Indeed, the C_{Hg}/C_{Hg}° was approximately 1 in each Region R1, R2 and R3, thus confirming that, under the adopted condition, the EK treatment using DW as processing fluid is not a viable way to desorb and mobilize Hg from the sediment. For each PAH, a similar distribution in the sediments was observed. In detail, the ratio C_i/C_i° increased from Region R3 to R2 and R1 for all the i-PAHs, and it was lower than 1 in all the regions ($C_i/C_i^\circ < 1$), except for BPR and IND (Figure 5, primary y-axis). In particular, a very similar distribution of FLU and PHE was observed: C_i/C_i° was 0.65, 0.55 and 0.44 in the case of FLU and 0.68, 0.58 and 0.50 in the case of PHE in Regions R1, R2 and R3, respectively. The lower content of i-PAHs in Region R3 suggests that they moved mainly from Region R3 to R1, where they were accumulated. In addition, some of these i-PAHs were partially removed from the sediments (total $R_i > 0\%$). Indeed, a R_i of both FLU and PHE slightly higher than 40% (Figure 5, secondary y-axis) was observed. The results were fully in line with the data reached in EK1 for PHE (Figure 3) using DW as processing fluid. Conversely, a very low total R_i value was observed of approximately 2.8% in the case of BPR and no removal of IND was reached (Figure 5). Overall, the higher the molecular weight (i.e., major number of aromatic rings), the lower the total R_i (Figure 5, secondary y-axis); this can be attributed to the different solubility of the five PAHs congeners [46], which results in different i-PAHs removal rate. The higher the molecular weight, the lower the solubility (FLU > PHE > BAP > BPR > IND), the lower the removal rate, resulting in $R_{PHE} > R_{FLU} > R_{BAP} > R_{BPR} > R_{IND}$. Overall, after the EK6 treatment, a total PAH removal, R_{PAHs}, of approximately 20% was reached under the adopted conditions (Table 3). These results could be rationalized by taking into consideration that PAHs are neutral-charged, nonpolar and hydrophobic compounds [14]. Hence, under the adopted condition, electromigration cannot be the main transport mechanism. Conversely, electroosmosis flow might be the only viable route for the mobilization of i-PAHs. In this case, electroosmosis flow moves from the cathode towards the anode side, according to Colacicco et al. [14], explaining the higher content of i-PAHs near the anode region (R1). However, their transport via electroosmotic flow is slow and tricky, due to their low water solubility and hydrophobicity. In addition, the total R_{PAHs} higher than zero indicates that PAHs were converted into other chemical compounds during the treatment. Hence, as already explained, during the EK treatment, the contaminants were desorbed and moved out from the sediments into the anode chamber, where they might be oxidized into other chemicals at the anode surface.

To improve the process performances, the best conditions achieved for the EK1-EK5 treatments of sediments contaminated with Hg and PHE were used for the treatment of the more complex matrix. Hence, DW was replaced with the T + MGDA solution as anolyte and MGDA solution as catholyte and the sediments spiked with Hg and the 5 PAHs congeners were treated at 1 V cm^{-1} using compact graphite as electrodes for 10 days (EK7). Also, in this case, at zero time, the contaminants were homogeneously distributed into the sediments placed inside the cell ($C_i/C_i^\circ \sim 1$) (Figure 6). After 10 days, as expected, C_{Hg}/C_{Hg}° was increased from R3 to R1 (Figure 6 refers primary y-axis) coupled with a total R_{Hg} of approximately 13%. This comportment was attributed to both the presence of MGDA, which creates negative Hg–organic charged complexes that migrated towards the positive electrode (Region R1—anode), and Tween 80, which aids the transport of Hg–organic complexes due to the presence of the soluble organic micelles. Moreover, under the adopted condition, the C_i/C_i° of the five PAHs congeners increases from R3 (cathode side) to R1 (anode side) and it was always lower than 1 (Figure 6 primary y-axis). This was coupled with a total R_i of each

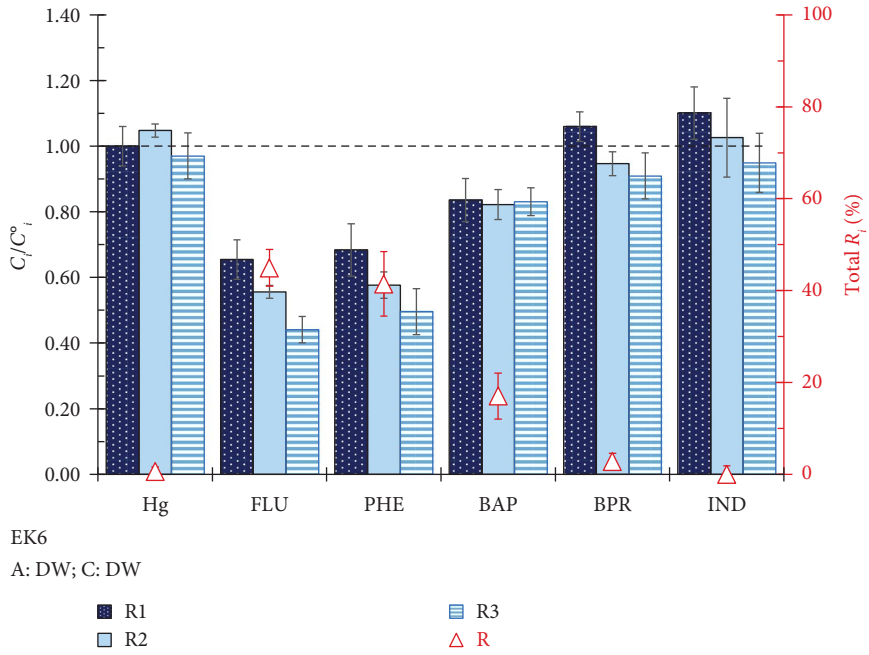

FIGURE 5: Final distribution of PAHs and Hg (C_i/C_i°) along the treated CG-MIX sediment (R1, R2 and R3) (primary x-axis) and their total removal R_i (refers to red triangle symbol, △, secondary y-axis) in the EK6 run. Black dashed line (---) indicates the initial normalized concentration ($C_i/C_i^\circ \sim 1$). A: Anolyte. C: Catholyte. DW: Deionized Water. Hg: Mercury. FLU: Fluorene. PHE: Phenanthrene. BAP: Benz(a)pyrene. BPR: Benzo(ghi)perylene. INP: Indeno(1,2,3-cd)pyrene. Electrolyses were performed under 1 V cm^{-1} for 10 days.

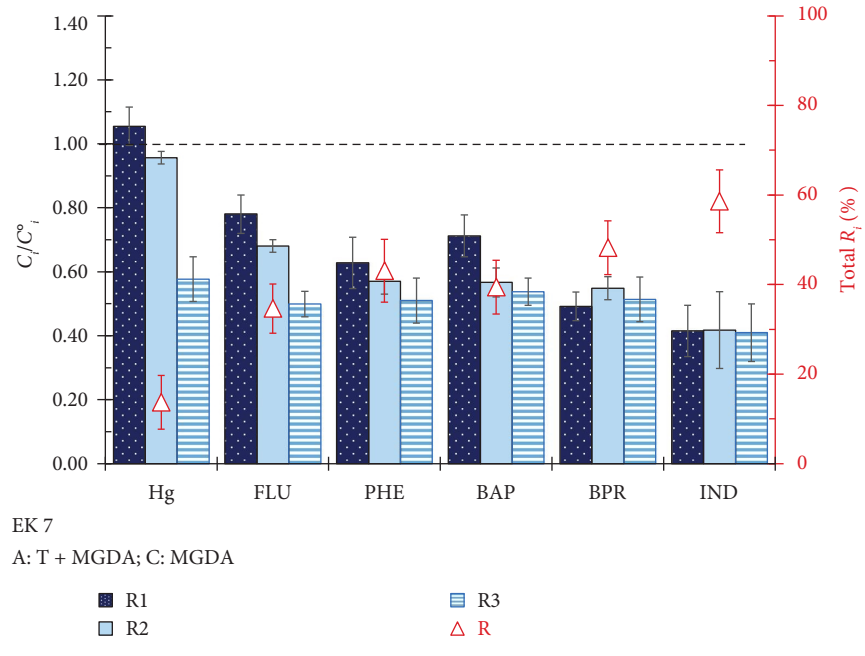

FIGURE 6: Final distribution of PAHs and Hg (C_i/C_i°) along the treated CG-MIX sediment (R1, R2 and R3) (primary x-axis) and their total removal R_i (refers to red triangle symbol, △, secondary y-axis) in the EK7 run. Black dashed line (---) indicates the initial normalized concentration ($C_i/C_i^\circ \sim 1$). A: Anolyte. C: Catholyte. MGDA: 0.1 M MGDA aqueous solution. T + MGDA: 3 g L^{-1} Tween 80 and 0.1 M MGDA aqueous solution. Hg: Mercury. FLU: Fluorene. PHE: Phenanthrene. BAP: Benz(a)pyrene. BPR: Benzo(ghi)perylene. INP: Indeno(1,2,3-cd)pyrene. Electrolyses were performed under 1 V cm^{-1} for 10 days.

contaminant higher than or equal to 40%. As an example, a total removal of BPR and IND R_{BPR} R_{IND} of approximately 48 and 58% was reached after 10 days, respectively. Overall, EK7 allowed to reach a total R_{PAHs} of 45% (Table 3, EK7), which is more than twice the R_{PAHs} reached using DW as processing fluid (Table 3, EK6). These results were attributed

Table 4: Comparison of electrochemical approaches for the remediation of soil or marine sediment contaminated by Hg and/or PAHs.

Entry	Matrix	Approach	Contaminants	E (V cm^{-1})	Electrodes	Time	R (%)	References
1	Contaminated clayed-sandy (Italy)	EK-A and C: 0.1 M KI at pH 3 continuously recirculated	Hg	Variable potentials between 25 and 60 V	Ti/Pt electrodes	Less than 3 months	60	[47]
2	Contaminated marine sediment	EK-A: 1 M NaOH C: 1 M HCl	Hg	20 V	MnO_2-coated Cu foam cathode	60 h	55	[48]
3	Marine sediments from Augusta Bay (Italy)	EK-A: MGDA + tween 80 C: 0.1 M EDTA Continuous electrolyte flow	PAHs	1.2	Stainless steel	10 days	60	[15]
4	Marine sediments from Augusta Bay (Italy)	EK-A: MGDA (5%) C: 0.1 M EDTA Continuous electrolyte flow	Hg	1.2	Stainless steel	400 h (~17 days)	38	[39]
5	Decommissioned gas plant soil (China)	EK-Fenton in situ production of H_2O_2	Three PAHs (anthracene, pyrene and benzanthracene)	1	Modified CMK3 gas diffusion electrodes	5 days	22–64	[24]
6	Spiked kaolin	EK-A and C: 1% Tween 80 and 0.1 M Na_2SO_4, controlling the catholyte pH at 7	Three PAHs (benzanthracene, fluoranthene, pyrene)	3	Graphite	23 days	~8	[46]
7	Spiked kaolin	EK-A and C: 1% Tween 80 and 0.1 M Na_2SO_4, controlling the anolyte pH at 7	Three PAHs (benzanthracene, fluoranthene, pyrene)	3	Graphite	23 days	39	[46]
8	Spiked marine sediment from Capo Granitola (Italy)	EK-A: 3 g·L^{-1} Tween 80 + 0.1 M MGDA C: 0.1 M MGDA; Batch electrolyte flow	PAHs Hg	1	Graphite	10 days	45 13	This work

to the presence of Tween 80 micelles, which create several zones that are highly soluble for PAHs congeners.

Finally, the results reached in the case of CG-MIX (EK7) were compared with corresponding literature data reported for EK remediation of low permeability soil and sediments contaminated by PAHs or Hg (Table 4). Overall, it was observed that the efficiency in the removal of PAHs and/or Hg significantly depends on the adopted operative conditions (such as induced *E*, time and enhancing agents) and on the nature of the treated solid sample.

4. Conclusions

Electrochemical remediation of marine sediments spiked with Hg and PAHs was systematically investigated to compare the effect of different electrolytes on the performance of the process. Hg and PHE or a mixture of five PAHs were adopted to spike real sediments dredged from CG coast (Italy) as model hazardous heavy metals and recalcitrant organics compounds. Overall, it was observed that the nature of the enhancing agents used as electrolytes and their combination strongly affect the remediation treatment distribution into the sediments and overall contaminants' removal.

DW processing of Hg is inefficient. Due to its chelating capabilities, using MGDA as an enhancing agent at the electrode compartments strongly changed the sediment Hg distribution. This leads to the formation of Hg–MGDA––organic complexes negatively charged which electromigrated towards the positive electrode. Moreover, the copresence of MGDA and a Tween 80 surfactant (T + MGDA) creates highly organic soluble micelles in which also the organic complexes could be solubilized and transported via electroosmosis to the electrode's compartments, aiding metal remediation and increasing Hg removal efficiency by 15–22.5%.

MGDA increases PHE removal efficiency by 36% compared to DW. Although it is well known that nonpolar molecules are not involved in the chelating process, these results can be due to a synergic transport phenomenon of electroosmosis and electromigration caused by the movement of the Hg–MGDA–organic complexes towards the anode compartment, enhancing the PHE transport.

Using MGDA and Tween 80 as anolytes (T + MGDA) and MGDA as catholytes was the best way to remove Hg, PHE or five PAHs simultaneously. These settings allow the maximum Hg and PHE removal of 22.5 and 62%, respectively, from sediments polluted with them. In sediments spiked with Hg and a mixture of five PAHs (FLU, PHE, BAP, BPR, IND), T + MGDA as anolyte and MGDA as catholyte removed 13% Hg and 45% PAHs.

Nomenclature

DCTs	Direct current technologies
SIN	Sites of National Interest
PAHs	Polycyclic aromatic hydrocarbons
PCBs	Polychlorinated biphenyls
TPHs	Total petroleum hydrocarbons
EK	Electrokinetics
ECRTs	Electrochemical remediation technologies
ECGO	Electrochemical geo-oxidation
MGDA	Trisodium N-(1-carboxylatoethyl)-iminodiacetate hydrate
Tween 80	Surfactant polyoxyethylene (20) sorbitan monooleate
EDTA	Ethylenediaminetetraacetic acid
CG	Capo Granitola Bay sediments (Trapani, Italy)
Hg	Mercury
PHE	Phenanthrene
FLU	Fluorene
BAP	Benz(a)pyrene
BPR	Benzo(ghi)perylene
INP	Indeno(1,2,3-cd)pyrene
HPLC	High-performance liquid chromatography
DW	Deionized water
DMA-80	Direct mercury analysers
ICP/MS	Inductively coupled plasma mass spectrometry
RSD	Relative standard deviation
GC/MS	Gas chromatography–mass spectrometry
R1	Region R1 section close to the anode side of the cell
R2	Region R2 section in the middle side of the cell
R3	Region R3 section close to the cathode side of the cell
CMC	Critical micellar concentration

Physical Symbols

C_i°	Initial *i*-contaminant concentration (mg kg^{-1})
C_i	Final *i*-contaminant concentration (mg kg^{-1})
C_i/C_i°	Normalized concentration of the final *i*-contaminant content (C_i) and the initial content (C_i°)
E	Electric field (V cm^{-1})
EC	Energetic consumption (kWh kg^{-1})
I	Current (mA)
R_i	Total removal from the sediments of the *i*-pollutant (%)
W	Moisture content (%)

Data Availability Statement

Data can be delivered if requested to the corresponding author via email.

Ethics Statement

The authors have nothing to report.

Disclosure

The authors have no relevant nonfinancial interests to disclose.

Conflicts of Interest

The authors declare no conflicts of interest.

Author Contributions

Federica Proietto: investigation, methodology, data curation, conceptualization, visualization, writing – original draft and review and editing; Claudia Prestigiacomo, Fabio D'Agostino and Maria Bonsignore: formal analysis and data curation; Mario Sprovieri: funding acquisition; Alessandro Galia: writing – review and editing and funding acquisition. Onofrio Scialdone: writing – review and editing, supervision and funding acquisition.

Funding

Partial financial support was received from MIUR PON "Ricerca & Competitività" 2007–2013 - Marine Hazard Project (cod. PON03PE_00203_1). Open access publishing was facilitated by University of Palermo as part of the CRUI-CARE agreement.

References

[1] K. R. Reddy and C. Cameselle, *Electro-Chemical Remediation Technologies for Polluted Soils, Sediments and Groundwater* (John Wiley & Sons, 2009).

[2] W. Chen, T. Xie, W. Li, and R. Wang, "Thinking of Construction of Soil Pollution Prevention and Control Technology System in China," *Acta Pedologica Sinica* 55 (2018): 557–568, https://doi.org/10.11766/trxb201711300488.

[3] Y. Song, D. Hou, J. Zhang, et al., "Environmental and Socio-Economic Sustainability Appraisal of Contaminated Land Remediation Strategies: A Case Study at a Mega Site in China," *Science of the Total Environment* 610-611 (2018): 391–401, https://doi.org/10.1016/j.scitotenv.2017.08.016.

[4] Y. B. Acar and A. N. Alshawabkeh, "Principles of Electrokinetic Remediation," *Environmental Science & Technology* 27, no. 13 (1993): 2638–2647, https://doi.org/10.1021/es00049a002.

[5] D. Wen, R. Fu, and Q. Li, "Removal of Inorganic Contaminants in Soil by Electrokinetic Remediation Technologies: A Review," *Journal of Hazardous Materials* 401 (2021): 123345, https://doi.org/10.1016/j.jhazmat.2020.123345.

[6] L. M. Zanko, J. K. Wittle, and S. Pamukcu, "Case Study: Electro-Chemical Geo-Oxidation (ECGO) Treatment of Massachusetts New Bedford Harbor Sediment PCBs," *Electrochimica Acta* 354 (2020): 136690, https://doi.org/10.1016/j.electacta.2020.136690.

[7] W. A. McIlvride, F. Doering, N. Doering, D. Hill, and J. L. Iovenitti, "Electrochemical Remediation Technologies for Metals Remediation in Soil, Sediment and Ground Water, Presentation of Case Histories," *Journal American Society of Mining and Reclamation* 2003, no. 1 (2003): 475–495, https://doi.org/10.21000/JASMR03010475.

[8] F. Proietto, A. Khalil, W. Maouch, A. Galia, and O. Scialdone, "Electrochemical Remediation of Phenol Contaminated Kaolin Under Low-Strength Electric Fields," *Environmental Technology & Innovation* 32 (2023): 103286, https://doi.org/10.1016/j.eti.2023.103286.

[9] F. Proietto, P. Meli, C. Prestigiacomo, A. Galia, and O. Scialdone, "Study of Electrochemical Remediation of Clay Spiked With C12-C18 Alkanes," *Journal of Environmental Chemical Engineering* 12, no. 1 (2024): 111780, https://doi.org/10.1016/j.jece.2023.111780.

[10] F. Proietto, F. D'Agostino, M. Bonsignore, et al., "Electrochemical Remediation of Synthetic and Real Marine Sediments Contaminated by PAHs, Hg and as Under Low Electric Field Values," *Chemosphere* 350 (2024): 141009, https://doi.org/10.1016/j.chemosphere.2023.141009.

[11] A. Saini, D. N. Bekele, S. Chadalavada, C. Fang, and R. Naidu, "Electrokinetic Remediation of Petroleum Hydrocarbon Contaminated Soil (I)," *Environmental Technology & Innovation* 23 (2021): 101585, https://doi.org/10.1016/j.eti.2021.101585.

[12] M. T. Alcántara, J. Gómez, M. Pazos, and M. A. Sanromán, "Combined Treatment of PAHs Contaminated Soils Using the Sequence Extraction With Surfactant–Electro-Chemical Degradation," *Chemosphere* 70, no. 8 (2008): 1438–1444, https://doi.org/10.1016/j.chemosphere.2007.08.070.

[13] M. T. Ammami, A. Benamar, H. Wang, et al., "Simultaneous Electrokinetic Removal of Polycyclic Aromatic Hydrocarbons and Metals From a Sediment Using Mixed Enhancing Agents," *International Journal of Environmental Science and Technology* 11, no. 7 (2014): 1801–1816, https://doi.org/10.1007/s13762-013-0395-9.

[14] A. Colacicco, G. De Gioannis, A. Muntoni, E. Pettinao, A. Polettini, and R. Pomi, "Enhanced Electrokinetic Treatment of Marine Sediments Contaminated by Heavy Metals and PAHs," *Chemosphere* 81, no. 1 (2010): 46–56, https://doi.org/10.1016/j.chemosphere.2010.07.004.

[15] P. P. Falciglia, D. Malarbì, V. Greco, and F. G. A. Vagliasindi, "Surfactant and MGDA Enhanced–Electrokinetic Treatment for the Simultaneous Removal of Mercury and PAHs From Marine Sediments," *Separation and Purification Technology* 175 (2017): 330–339, https://doi.org/10.1016/j.seppur.2016.11.046.

[16] A. Gharaee, M. R. Khosravi-Nikou, and B. Anvaripour, "Hydrocarbon Contaminated Soil Remediation: A Comparison Between Fenton, Sono-Fenton, Photo-Fenton and Sono-Photo-Fenton Processes," *Journal of Industrial and Engineering Chemistry* 79 (2019): 181–193, https://doi.org/10.1016/j.jiec.2019.06.033.

[17] R. Iannelli, M. Masi, A. Ceccarini, et al., "Electrokinetic Remediation of Metal-Polluted Marine Sediments: Experimental Investigation for Plant Design," *Electrochimica Acta* 181 (2015): 146–159, https://doi.org/10.1016/j.electacta.2015.04.093.

[18] G. Lofrano, G. Libralato, D. Minetto, et al., "In Situ Remediation of Contaminated Marine Sediment: An Overview," *Environmental Science & Pollution Research* 24, no. 6 (2017): 5189–5206, https://doi.org/10.1007/s11356-016-8281-x.

[19] D. Malarbì, P. P. Falciglia, and F. G. A. Vagliasindi, "Removal of Hg From Real Polluted Sediments Using Enhanced-EK Decontamination: Verification of Experimental Methods and Batch-Test Preliminary Results," *Journal of Chemistry* (2015): 270451, https://doi.org/10.1155/2015/270451.

[20] M. Pazos, E. Rosales, T. Alcántara, J. Gómez, and M. A. Sanromán, "Decontamination of Soils Containing PAHs by Electroremediation: A Review," *The Journal of Hazardous Materials* 177, no. 1-3 (2010): 1–11, https://doi.org/10.1016/j.jhazmat.2009.11.055.

[21] M. Pazos, O. Iglesias, J. Gómez, E. Rosales, and M. A. Sanromán, "Remediation of Contaminated Marine Sediment Using Electrokinetic–Fenton Technology," *Journal of Industrial and Engineering Chemistry* 19, no. 3 (2013): 932–937, https://doi.org/10.1016/j.jiec.2012.11.010.

[22] J. Wang, X. Feng, C. W. N. Anderson, Y. Xing, and L. Shang, "Remediation of Mercury Contaminated Sites–A Review," *Journal of Hazardous Materials* 221–222 (2012): 1–18, https://doi.org/10.1016/j.jhazmat.2012.04.035.

[23] M. Cheng, G. Zeng, D. Huang, et al., "Advantages and Challenges of Tween 80 Surfactant-Enhanced Technologies for the Remediation of Soils Contaminated With Hydrophobic Organic Compounds," *Chemical Engineering Journal (1996)* 314 (2017): 98–113, https://doi.org/10.1016/j.cej.2016.12.135.

[24] L. Chu, L. Cang, G. Fang, et al., "A Novel Electrokinetic Remediation With In-Situ Generation of H_2O_2 for Soil PAHs Removal," *Journal of Hazardous Materials* 428 (2022): 128273, https://doi.org/10.1016/j.jhazmat.2022.128273.

[25] N. Porcino, F. Crisafi, M. Catalfamo, R. Denaro, and F. Smedile, "Electrokinetic Remediation in Marine Sediment: A Review and a Bibliometric Analysis," *Sustainability (Basel)* 16, no. 11 (2024): 4616, https://doi.org/10.3390/su16114616.

[26] S. Barba, R. López-Vizcaíno, C. Saez, et al., "Electro-Bioremediation at the Prototype Scale: What it Should Be Learned for the Scale-Up," *Chemical Engineering Journal (1996)* 334 (2018): 2030–2038, https://doi.org/10.1016/j.cej.2017.11.172.

[27] Y. Gong, D. Zhao, and Q. Wang, "An Overview of Field-Scale Studies on Remediation of Soil Contaminated With Heavy Metals and Metalloids: Technical Progress Over the Last Decade," *Water Research* 147 (2018): 440–460, https://doi.org/10.1016/j.watres.2018.10.024.

[28] E. K. Jeon, J. M. Jung, W. S. Kim, S. H. Ko, and K. Baek, "In Situ Electrokinetic Remediation of As-Cu-And Pb-Contaminated Paddy Soil Using Hexagonal Electrode Configuration: A Full Scale Study," *Environmental Science & Pollution Research* 22, no. 1 (2015): 711–720, https://doi.org/10.1007/s11356-014-3363-0.

[29] D. Han, X. Wu, R. Li, X. Tang, S. Xiao, and M. Scholz, "Critical Review of Electro-Kinetic Remediation of Contaminated Soils and Sediments: Mechanisms, Performances and Technologies," *Water, Air, and Soil Pollution* 232, no. 8 (2021): 335, https://doi.org/10.1007/s11270-021-05182-4.

[30] R. López-Vizcaíno, V. Navarro, J. Alonso, et al., "Geotechnical Behaviour of Low-Permeability Soils in Surfactant-Enhanced Electrokinetic Remediation," *Journal of Environmental Science and Health, Part A* 51, no. 1 (2016): 44–51, https://doi.org/10.1080/10934529.2015.1079106.

[31] R. López-Vizcaíno, V. Navarro, M. J. León, et al., "Scale-up on Electrokinetic Remediation: Engineering and Technological Parameters," *Journal of Hazardous Materials* 315 (2016): 135–143, https://doi.org/10.1016/j.jhazmat.2016.05.012.

[32] R. López-Vizcaíno, C. Risco, J. Isidro, et al., "Scale-Up of the Electrokinetic Fence Technology for the Removal of Pesticides. Part II: Does Size Matter for Removal of Herbicides," *Chemosphere* 166 (2017): 549–555, https://doi.org/10.1016/j.chemosphere.2016.09.114.

[33] R. López-Vizcaíno, A. Yustres, C. Sáez, et al., "Techno-Economic Analysis of the Scale-Up Process of Electrochemically-Assisted Soil Remediation," *Journal of Environmental Management* 231 (2019): 570–575, https://doi.org/10.1016/j.jenvman.2018.10.084.

[34] D. Huguenot, E. Mousset, E. D. van Hullebusch, and M. A. Oturan, "Combination of Surfactant Enhanced Soil Washing and Electro-Fenton Process for the Treatment of Soils Contaminated by Petroleum Hydrocarbons," *Journal of Environmental Management* 153 (2015): 40–47, https://doi.org/10.1016/j.jenvman.2015.01.037.

[35] O. Scialdone, F. Proietto, and A. Galia, "Electrochemical Production and Use of Chlorinated Oxidants for the Treatment of Wastewater Contaminated by Organic Pollutants and Disinfection," *Current Opinion in Electrochemistry* 27 (2021): 100682, https://doi.org/10.1016/j.coelec.2020.100682.

[36] S. Randazzo, A. Geagea, F. Proietto, A. Galia, and O. Scialdone, "Oxidation of Organics in Water by Active Chlorine Performed in Microfluidic Electrochemical Reactors: A New Way to Improve the Performances of the Process," *Chemosphere* 355 (2024): 141855, https://doi.org/10.1016/j.chemosphere.2024.141855.

[37] Y. Hao, H. Ma, F. Proietto, A. Galia, and O. Scialdone, "Electrochemical Treatment of Wastewater Contaminated by Organics and Containing Chlorides: Effect of Operative Parameters on the Abatement of Organics and the Generation of Chlorinated By-Products," *Electrochimica Acta* 402 (2022): 139480, https://doi.org/10.1016/j.electacta.2021.139480.

[38] J. Jachuła, D. Kołodynska, and Z. Hubicki, "Sorption of Zn(II) and Pb(II) Ions in the Presence of the Biodegradable Complexing Agent of a New Generation," *Chemical Engineering Research and Design* 90 (2012): 1671–1679, https://doi.org/10.1016/j.cherd.2012.01.015.

[39] P. P. Falciglia, D. Malarbì, and F. G. A. Vagliasindi, "Removal of Mercury From Marine Sediments by the Combined Application of a Biodegradable Non-Ionic Surfactant and Complexing Agent in Enhanced-Electrokinetic Treatment," *Electrochimica Acta* 222 (2016): 1569–1577, https://doi.org/10.1016/j.electacta.2016.11.142.

[40] C. Prieto and L. Calvo, "Performance of the Biocompatible Surfactant Tween 80, for the Formation of Microemulsions Suitable for New Pharmaceutical Processing," *Journal of Applied Chemistry* 2013 (2013): 1–10, https://doi.org/10.1155/2013/930356.

[41] I. C. Paixão, R. López-Vizcaíno, A. M. S. Solano, et al., "Electrokinetic-Fenton for the Remediation Low Hydraulic Conductivity Soil Contaminated With Petroleum," *Chemosphere* 248 (2020): 126029, https://doi.org/10.1016/j.chemosphere.2020.126029.

[42] M. Ni, S. Tian, Q. Huang, and Y. Yang, "Electrokinetic-Fenton Remediation of Organochlorine Pesticides From Historically Polluted Soil," *Environmental Science & Pollution Research* 25, no. 12 (2018): 12159–12168, https://doi.org/10.1007/s11356-018-1479-3.

[43] P. Ma, C. Prestigiacomo, F. Proietto, A. Galia, and O. Scialdone, "Electrochemical Treatment of Wastewater by Electro Fenton, Photo-Electro Fenton, Pressurized-Electro Fenton and Pressurized Photo Electro Fenton: A First Comparison of These Innovative Routes," *Chemelectrochem* 8, no. 16 (2021): 3135–3142, https://doi.org/10.1002/celc.202100736.

[44] S. Sabatino, C. Prestigiacomo, F. Proietto, A. Galia, E. Petrucci, and O. Scialdone, "Effect of the Pressure on the Cathodic Production of H_2O_2 and on Electro-Fenton in Undivided and Divided Cells," *Journal of Water Process Engineering* 61 (2024): 105297, https://doi.org/10.1016/j.jwpe.2024.105297.

[45] N. Hamdi, F. Proietto, H. Ben Amor, et al., "Effective Removal and Mineralization of 8-hydroxyquinoline-5-sulfonic Acid Through a Pressurized electro-Fenton-Like Process With Ni–Cu–Al Layered Double Hydroxide," *Chemelectrochem* 7,

no. 11 (2020): 2457–2465, https://doi.org/10.1002/celc.202000463.

[46] M. T. Alcántara, J. Gómez, M. Pazos, and M. A. Sanromán, "Electrokinetic Remediation of PAH Mixtures From Kaolin," *Journal of Hazardous Materials* 179, no. 1-3 (2010): 1156–1160, https://doi.org/10.1016/j.jhazmat.2010.03.010.

[47] D. Rosestolato, R. Bagatin, and S. Ferro, "Electrokinetic Remediation of Soils Polluted by Heavy Metals (Mercury in Particular)," *Chemical Engineering Journal (1996)* 264 (2015): 16–23, https://doi.org/10.1016/j.cej.2014.11.074.

[48] C. Bunditboondee, J. Lohwacharin, E. Khan, S. Kulyakoon, and K. Laohhasurayotin, "Effects of Cathode Coating Materials and Operational Time on the Mercury Removal Performance of Electrokinetic Remediation System for Marine Sediment," *Journal of Environmental Management* 288 (2021): 112443, https://doi.org/10.1016/j.jenvman.2021.112443.